
Neural Active Learning Meets the Partial Monitoring Framework

Maxime Heuillet¹

Ola Ahmad^{1,3}

Audrey Durand^{1,2}

¹Université Laval, Canada

²Canada-CIFAR AI Chair, Mila, Canada

³Thales Research and Technology (cortAIx), Canada,

Abstract

We focus on the online-based active learning (OAL) setting where an agent operates over a stream of observations and trades-off between the costly acquisition of information (labelled observations) and the cost of prediction errors. We propose a novel foundation for OAL tasks based on partial monitoring, a theoretical framework specialized in online learning from partially informative actions. We show that previously studied binary and multi-class OAL tasks are instances of partial monitoring. We expand the real-world potential of OAL by introducing a new class of cost-sensitive OAL tasks. We propose `NeuralCBP`, the first PM strategy that accounts for predictive uncertainty with deep neural networks. Our extensive empirical evaluation on open source datasets shows that `NeuralCBP` is competitive with, and even outperforms state-of-the-art baselines on multiple binary, multi-class and cost-sensitive OAL tasks.

1 INTRODUCTION

In active learning [Cohn et al., 1994], an agent decides to query an expert to obtain labels on selected observations. This active acquisition of labels efficiently reduces the number of labelled observations needed to learn a task. Active learning therefore appears as a cost-effective solution for modern machine learning, which often relies on large volumes of labelled observations [Kusne et al., 2020].

In this work, we focus on the *online-based active learning* (OAL) setting for binary and multi-class classification tasks Beygelzimer et al. [2009]. The agent operates over a (possibly infinite) stream of observations. For each observation, the agent predicts the class and either decides to reveal its prediction or to query an expert to obtain the label. The OAL setting we consider differs from the *batch setting* where the

agent gathers fixed-size batches of observations to label Saran et al. [2023], Amin et al. [2020]. In both the OAL and the batch-based settings, all decisions are irrevocable and associated with costs. The goal is to minimize the cumulative cost over the stream of decisions, by trading-off between the cost of obtaining new labels (*labeling complexity*) and the cost of prediction errors (*generalization performance*).

In the context of OAL for binary classification, the `Margin` strategy [Sculley, 2007] queries the expert when the prediction uncertainty is greater than a user-specified threshold. In contrast, with `Cesa` [Cesa-Bianchi et al., 2006], labelled observations are acquired proportionally to the global prediction error rate of the strategy. Both `Margin` and `Cesa` are specifically analyzed for the class of linear separators and are designed for binary tasks. More recent studies focused on multi-class OAL tasks. The `Gapplettron` [van der Hoeven et al., 2021] leverages graph feedback, making it inherently multi-class. However, similarly to `Cesa` and `Margin`, `Gapplettron` is specifically analyzed for linear separators.

Modern applications of machine learning involve high-dimensional observations that require learning complex representations. As a result, `Neural` [Wang et al., 2021] and `ALPS` [DeSalvo et al., 2021] proposed multi-class OAL strategies based on deep neural networks. `Neural` and `ALPS` have been outperformed by `INeural` [Ban et al., 2022b], an improved and more practical version of the `Neural` strategy [Wang et al., 2021]. The current state-of-the-art, `Neuronal` [Ban et al., 2024], addresses scalability limitations of `INeural`, opening the door to using sophisticated neural architectures, such as convolutional neural networks.

In critical real-world applications, the costs of prediction errors from one class to another may vary significantly. Cost-sensitive OAL is studied for regression tasks [Cai et al., 2023], but classification tasks remain an open problem. Existing OAL strategies all assume *uniform costs*, i.e. prediction error and labeling costs are the same across all classes. This assumption is the core of the algorithmic design of ex-

isting approaches, making it challenging to extend them to cost-sensitive tasks. Motivated by the fact that cost-sensitive learning has fostered the adoption of supervised learning in real-world scenarios, such as learning from imbalanced data [Elkan, 2001], we address the following questions: *1) How to frame cost-sensitive OAL classification tasks? and, 2) Can we design a practical cost-sensitive OAL agent?*

Contributions. We tackle these questions from a novel perspective based on Partial Monitoring (PM) [Piccolboni et al., 2001, Bartók et al., 2014], a theoretical framework for online learning problems with partially informative actions. ① *Connecting ideas in separate fields:* We hypothesize and validate that we can establish a novel, non-trivial, connection between the field of active learning and the PM framework. ② *Methodological:* We show how partial monitoring reduces to existing binary and multi-class OAL tasks and enables the formulation of novel cost-sensitive OAL tasks. ③ *Algorithmic:* We propose `NeuralCBP` (Neural Confidence Bound Partial Monitoring), the first neural partial monitoring (PM) strategy. Existing PM strategies are limited to the linear [Heuillet et al., 2024] and logistic [Bartók et al., 2012a], which constitute a bottleneck towards the adoption of PM in practice. `NeuralCBP` presents algorithmic dynamics that differ from existing OAL strategies, which can be of independent interest to the OAL community. ④ *Empirical:* Our empirical evaluation shows that `NeuralCBP` competes with, and even outperforms the current state-of-the-art in multiple binary and multi-class settings, and across various neural architectures. ⑤ *Advocacy:* Documented applied studies of PM are restricted to synthetic experiments Singla et al. [2014], Kirschner et al. [2023], Heuillet et al. [2024] and PM traditionally has been more supported by theoretical advances. Our work is the first to showcase that PM can be effectively applied in real-world scenarios such as OAL, highlighting its potential and encouraging its adoption. ⑥ *Reproducibility:* To support further adoption, we make our study fully reproducible with open-source code for the strategies and evaluation environments. Appendix A shows how to instantiate the complex formal definitions of the PM framework.

2 BACKGROUND

A PM [Bartók et al., 2014] game is played between a learning agent and the environment over multiple rounds. The agent has a finite set of N actions. The environment has a finite set of M outcomes. The game is defined by a cost matrix $\mathbf{C} \in [0, 1]^{N \times M}$ and a feedback matrix $\mathbf{H} \in \Sigma^{N \times M}$. The symbol space Σ is arbitrary and is not necessarily numeric (i.e. could be symbols). Without loss of generality, we assume that feedback symbols associated with one action are distinct from those induced by the other actions. We note \mathbf{c}_i the i -th row of the matrix \mathbf{C} . The same notation applies to matrix \mathbf{H} . A summary table of the important notations is reported in Table 1 in the Appendix.

2.1 DYNAMICS OF A GAME

Matrices \mathbf{C} and \mathbf{H} are revealed to the agent before the game begins. The horizon of rounds T is unknown to the agent. At each round $t \in \{1, 2, \dots, T\}$, the environment samples an observation $x_t \in \mathcal{X}$. We make no assumption regarding the sampling process of the observations. The environment then samples an outcome $y_t \in \{1, 2, \dots, M\}$ from an *outcome distribution* that depends on x_t , and that is denoted $p(x_t) \in \Delta_M \subset \mathbb{R}^{M \times 1}$, where Δ_M is the M -dimensional probability simplex. We assume outcomes are sampled i.i.d with respect to the outcome distribution.

The agent observes x_t and selects an action $i_t \in \{1, 2, \dots, N\}$. Then, the agent then incurs a cost $\mathbf{C}[i_t, y_t]$ and receives a feedback symbol $h_t = \mathbf{H}[i_t, y_t]$, where $[i, y]$ denotes the element at row i and column y . Therefore, costs and feedback symbols are deterministic elements of matrices \mathbf{C} and \mathbf{H} respectively. We emphasize that the agent only observes the feedback symbol h_t , with neither the outcome nor the cost being revealed.

The goal is to minimize the cost incurred in each round. This is achieved by selecting the action i_t^* that minimizes the expected cost for x_t , and is defined such that $i_t^* = \operatorname{argmin}_{1 \leq i \leq N} \mathbf{c}_i p(x_t)$. The performance of the agent is measured by the cumulative regret (to minimize) w.r.t. the optimal action strategy:

$$R(T) = \sum_{t=1}^T (\mathbf{c}_{i_t} - \mathbf{c}_{i_t^*}) p(x_t), \quad (1)$$

Eq. 1 scales sub-linearly with T if the agent identifies the optimal action and commits to it over time. This requires to balance *exploration* (playing informative actions) and *exploitation* (minimizing per-round regret).

2.2 STRUCTURE OF A GAME

We now introduce two definitions to characterize the cost \mathbf{C} and feedback \mathbf{H} matrices of any PM game.

Definition 2.1 (Cell decomposition, Bartók et al. [2012b]). The *cell* \mathcal{O}_i is defined as the subspace in the probability simplex Δ_M such that action i would be optimal. Formally, $\mathcal{O}_i = \{p \in \Delta_M, \forall j \in \{1, \dots, N\}, (\mathbf{c}_i - \mathbf{c}_j)p \leq 0\}$.

Based on the above definition, action i is: (i) *dominated* if $\mathcal{O}_i = \emptyset$ (i.e. there is no outcome distribution s.t. the action is optimal); (ii) *degenerate* if it is not dominated and there exist action k such that $\mathcal{O}_i \subsetneq \mathcal{O}_k$ (i.e. actions i and k are duplicates, both are jointly optimal under some outcome distribution); and (iii) *Pareto-optimal* otherwise. The set of Pareto-optimal actions is denoted \mathcal{P} .

For an action i , let σ_i denote the number of unique feedback symbols on \mathbf{h}_i . Let $\Sigma_i = \{s_1, \dots, s_{\sigma_i}\}$ denote the enumeration of symbols sorted by order of appearance in \mathbf{h}_i . Let $\pi_i(x_t) \in \Delta_{\sigma_i} \subset \mathbb{R}^{\sigma_i \times 1}$ denote the probability distribution of receiving each feedback symbol of action i given x_t .

Definition 2.2 (Signal matrix, Bartók et al. [2012b]). Given action i , the elements in the *signal matrix* $S_i \in \{0, 1\}^{\sigma_i \times M}$ are defined as $S_i[u, v] = \mathbb{1}_{\{\mathbf{H}[i, v] = s_u\}}$.

Property 2.3. *The outcome distribution is connected to the feedback symbols distribution of action i through the signal matrix S_i with the relation $\pi_i(x_t) = S_i p(x_t)$.*

3 STREAM-BASED ACTIVE LEARNING AS A PARTIAL MONITORING GAME

We now explain how to formulate OAL classification tasks under a class of PM games, known as *label-efficient* games. The original label-efficient game [Helmbold et al., 1997] is characterized by $N = 3$ actions (predict class 1, predict class 2, and query the expert), $M = 2$ outcomes (the ground-truth classes), and the following cost and feedback matrices:

$$\mathbf{C} = \begin{array}{c} \text{pred. class 1} \\ \text{pred. class 2} \\ \text{expert} \end{array} \begin{array}{cc} \text{class 1} & \text{class 2} \\ \left[\begin{array}{cc} 0 & 1 \\ 1 & 0 \\ 1 & 1 \end{array} \right] \end{array}, \mathbf{H} = \begin{array}{cc} \text{class 1} & \text{class 2} \\ \left[\begin{array}{cc} \diamond & \diamond \\ \wedge & \wedge \\ \perp & \odot \end{array} \right] \end{array}.$$

For reproducibility, in Appendix A, we instantiate all the definitions presented above using the label-efficient game as an example. Several OAL studies on binary classification correspond to instances of the original label-efficient game [Cohn et al., 1994, Balcan et al., 2007, Beygelzimer et al., 2009].

Using the game theoretical definitions presented above and developed in Bartók et al. [2012b], we now introduce a generalization of this game to multi-class classification with possibly non-uniform costs and multiple experts.

Generalized label-efficient game The OAL classification task with M classes and E experts can be cast as a PM game with $N = M + E$ actions and M outcomes. Without loss of generality, we assume that the actions $\{M + 1, \dots, M + E\}$ correspond to requesting a label from the $E \geq 1$ experts. All actions $i > M$ (i.e. actions associated with an expert) are *dominated* (see Def. 2.1) and admit $\sigma_i = M$ distinct symbols. The other actions $\{1, \dots, M\}$ lead to a single feedback symbol, i.e. $\sigma_i = 1$.

The original label-efficient game corresponds to the single-expert ($E = 1$) binary task ($M = 2$) with a uniform cost matrix. In this work, we focus on single-expert multi-class ($M \geq 2$) games with a potentially non-uniform cost matrix. The multi-expert setting ($E > 1$) suggests that experts reveal the outcome (ground-truth label) with different stochasticity levels. Capturing this would require a different PM setting where feedback is subject to noise, as studied by Kirschner et al. [2020, 2023].

Connecting regret minimization and OAL The cost matrix captures both the cost of querying an expert and the cost

of prediction errors. The goal of PM agents is to minimize the regret (see Eq. 1), which corresponds to simultaneously minimizing the cost associated with label queries (label complexity) and the cost of prediction errors (generalization performance). This goal aligns with the objectives of established OAL methodologies [DeSalvo et al., 2021, Wang et al., 2021, Ban et al., 2022b, 2024].

4 THE NEURALCBP APPROACH

We now introduce `NeuralCBP`, the first partial monitoring strategy able to learn from neural networks. While the emphasis of this study is on OAL classification tasks, `NeuralCBP` is a general PM strategy that can be applied to the broader diversity of PM games. Algorithm 1 displays the pseudo-code of `NeuralCBP`.

The proposed `NeuralCBP` builds upon `CBP` (Confidence Bound Partial Monitoring) methods Bartók et al. [2012b], which currently have limited practical potential due to linear [Heuillet et al., 2024] and logistic [Bartók et al., 2012a] model assumptions. For an observation x_t , the expected cost difference between two actions i and j is

$$\delta_{i,j}(x_t) = (\mathbf{c}_i - \mathbf{c}_j)p(x_t), \quad (2)$$

where $p(x_t)$ is unknown by definition of the PM game. Action j is better than action i when $\delta_{i,j}(x_t) > 0$.

Definition 4.1 (Neighbors, Bartók et al. [2012b]). Two Pareto-optimal actions i and j are *neighbors* if $\mathcal{O}_i \cap \mathcal{O}_j$ is a $(M - 2)$ -dimensional polytope. The set of all neighbor pairs is denoted \mathcal{N} .

Two actions are neighbors when these actions can not be jointly optimal for a given outcome distribution. Therefore, given observation x_t , one only needs to compute $\delta_{i,j}(x_t)$ for neighbor pairs in \mathcal{N} at round t , rather than for all the action pairs $\{i, j\}$ in the game [Bartók et al., 2012b].

4.1 OUTCOME AND FEEDBACK DISTRIBUTIONS

Recall that the agent does not observe the outcomes. Consequently, the agent cannot directly estimate the outcome distribution $p(x_t)$. As a result, estimating the expected cost difference $\delta_{i,j}(x_t)$ using Eq. 2 is not feasible in practice. This motivates additional definitions to estimate the expected loss difference in practice.

Definition 4.2 (Observer set, Bartók et al. [2012b]). The set $V_{i,j}$ includes all actions that verify the relation $(\mathbf{c}_i - \mathbf{c}_j)^\top \in \bigoplus_{a \in V_{i,j}} \text{Im}(S_a^\top)$, where \bigoplus corresponds to the direct sum.

Definition 4.3 (Observer vectors, Bartók et al. [2012b]). Given action $a \in V_{i,j}$, the observer vector $v_{ija} \in \mathbb{R}^{\sigma_a}$ is selected to satisfy the relation $(\mathbf{c}_i - \mathbf{c}_j)^\top = \sum_{a \in V_{i,j}} S_a^\top v_{ija}$.

Algorithm 1: NeuralCPB

input : \mathcal{P}, \mathcal{N}

```

1 Initialize  $\theta_1, \theta_2$ 
2  $G_{a,t} = \lambda \mathbf{1}_{m+\sigma m}, \forall a \in \{1, \dots, N\}$ 
3 for  $t > N$  do
4   Initialize  $\mathcal{U}(t) \leftarrow \{\}$ 
5   Receive observation  $x_t$ 
6   Get  $\hat{\pi}(x_t)$  based on  $f_1(x_t, \theta_1)$ 
7   Get  $w(x_t)$  based on  $f_2(x_t, \theta_2)$ 
8   for each action-pair  $\{i, j\} \in \mathcal{N}$  do
9      $\hat{\delta}_{i,j}(t) = \sum_{a \in V_{i,j}} v_{ija} \hat{\pi}_a(x_t)$ 
10     $z_{i,j}(t) \leftarrow \sum_{a \in V_{i,j}} \|v_{ija}\|_2 w_a(x_t)$ 
11    if  $|\hat{\delta}_{i,j}(t)| \geq z_{i,j}(t)$  then
12      | Add  $\{i, j\}$  to  $\mathcal{U}(t)$ 
13  Compute  $D(t)$  based on  $\mathcal{U}(t)$ 
14  Obtain  $\mathcal{P}(t)$  and  $\mathcal{N}(t)$  based on  $D(t)$ 
15   $\mathcal{N}^+(t) \leftarrow \bigcup_{i,j \in \mathcal{N}(t)} \mathcal{N}_{i,j}^+$ 
16   $\mathcal{V}(t) \leftarrow \bigcup_{i,j \in \mathcal{N}(t)} V_{i,j}$ 
17  Compute  $\mathcal{R}(x_t)$ 
18   $\mathcal{S}(t) \leftarrow \mathcal{P}(t) \cup \mathcal{N}^+(t) \cup (\mathcal{V}(t) \cap \mathcal{R}(x_t))$ 
19  Play  $a_t = \operatorname{argmax}_{a \in \mathcal{S}(t)} W_a w_a(x_t)$ 
20  Observe feedback  $h_t$ 
21  Update  $\theta_1, \theta_2$  with Algorithm 2 (Appendix B)
22  Update  $G_{a,t}^{-1}$  (see Sherman et al. [1950])

```

The set $V_{i,j}$ contains actions that induce informative feedback symbols about $\mathbf{c}_i - \mathbf{c}_j$. It is defined such that $\mathbf{c}_i - \mathbf{c}_j$ can be expressed as a linear combination of the signal matrix images of actions in $V_{i,j}$, with the observer vectors being the coefficients of the combination.

Combining Definitions 4.2 and 4.3 with Property 2.3 allows to express $\delta_{i,j}(x_t)$ as a function of the feedback distributions $\pi_a(x_t)$ of all actions $a \in V_{i,j}$:

$$\delta_{i,j}(x_t) = \sum_{a \in V_{i,j}} v_{ija}^\top \pi_a(x_t). \quad (3)$$

Consequently, one can compute the estimate $\hat{\delta}_{i,j}(x_t)$ using the feedback distribution estimates $\hat{\pi}_a(x_t)$ associated with the actions in $V_{i,j}$. Similarly, the uncertainty in the loss difference estimate $\hat{\delta}_{i,j}(x_t)$ is:

$$z_{i,j}(x_t) = \sum_{a \in V_{i,j}} \|v_{ija}\|_\infty w_a(x_t), \quad (4)$$

where $w_a(x_t)$ is the uncertainty on $\hat{\pi}_a(x_t)$ [Lienert, 2013]. Methods to compute $\hat{\pi}_a(x_t)$ and $w_a(x_t)$ depend on the setting considered, e.g. without side-observation Bartók et al. [2012b], or with linear Heuillet et al. [2024], or logistic Bartók et al. [2014] side-information. We now present a method for the neural setting.

4.2 INFERENCE WITH NEURAL NETWORKS

The strategy INeural [Ban et al., 2022b] frames the OAL classification task under bandit feedback, where all actions are self-informative. As a result, INeural leverages the Explore-Exploit Networks (referred to as EENets) initially introduced for bandit feedback [Ban et al., 2022a]. The current state-of-the-art in OAL (Neuronal [Ban et al., 2024]), is a follow-up strategy based on EENets that showcases the limitations of a bandit feedback structure and highlights the importance of finding an adequate and general feedback structure for the diversity of OAL classification tasks. As a response, we extend EENets to address the exploration-exploitation trade-off in the general PM setting. This extension is non-trivial because the PM feedback/cost structure requires exploration techniques that go beyond techniques used in bandit feedback. Further technical differences between NeuralCBP and other EENets strategies are discussed in Section 6.

EENets comprise an *exploitation network* (denoted f_1) to estimate action values and an *exploration network* (denoted f_2) to quantify the uncertainty on the predictions of f_1 .

Exploitation network In the PM setting, the exploitation network f_1 predicts the feedback distributions required in Eq. 3. To instantiate efficiently the exploitation network f_1 in PM, we need to distinguish informative from non-informative actions.

Definition 4.4 (Set of informative actions). The set of informative actions, $\mathcal{I} = \{i : i \in \{1, \dots, N\}, \text{ and } \sigma_i \geq 2\}$, comprises all actions that induce at least two distinct feedback symbols.

Definition 4.5 (Valid feedback symbols). The set of valid feedback symbols is noted $\Sigma_{\mathcal{I}} = \bigcup_{i \in \mathcal{I}} \Sigma_i$. The dimension of $\Sigma_{\mathcal{I}}$ is $\sigma = \sum_{i \in \mathcal{I}} \sigma_i$, which represents the total number of unique symbols induced by the actions in \mathcal{I} .

Current CBP strategies Bartók et al. [2012a], Lienert [2013], Heuillet et al. [2024] estimate the feedback distribution for all the actions of a game. However, Property 2.3 shows that for any uninformative action $i \notin \mathcal{I}$, the learned feedback distribution is always $\pi_i(x_t) = 1$. In some PM games, most of the actions are uninformative, as it is the case for *generalized label-efficient* games (presented in Section 3) where only expert actions are informative. Therefore, attributing learnable parameters to uninformative actions, as is done in current CBP strategies [Heuillet et al., 2024, Bartók et al., 2012a], turns out to be inefficient. In contrast, NeuralCBP attributes learnable parameters only to the informative actions in the game (see Definition 4.4). Restricting learnable parameters to the subset of informative actions \mathcal{I} is essential because NeuralCBP relies on the Explore-Exploit networks (EENets) that require a shared representation for

the actions. Including non-informative actions would cause overfitting, unstable learning, and increased complexity.

Definition 4.6 (Set of informative feedback distributions). The set of informative feedback distributions, denoted $\Pi(x_t) = \{\pi_i(x_t), i \in \mathcal{I}\}$, contains the (unknown) feedback distribution vectors of each informative action.

Remark 4.7. For practical purposes, remark that the set $\Pi(x_t)$ can be converted into a (flattened) σ -dimensional row vector. The conversion from a set to a flattened vector, and conversely from a flattened vector to a set, is possible because the cardinality σ_i of each feedback distribution is known by definition of the PM game.

The network f_1 , therefore, learns the flattened vector associated with $\Pi(x_t)$ and predicts the desired estimates $\hat{\pi}_i(x_t)$ for actions $i \in \mathcal{I}$. Network f_1 can be instantiated as a fully connected multi-layer perceptron of depth L and width m :

$$f_1(x_t, \theta_1) = W_1^L \Psi(W_1^{L-1} \Psi(W_1^{L-2} \dots \Psi(W_1^1 x_t))),$$

where $W_1^1 \in \mathbb{R}^{m \times d}$, $W_1^\ell \in \mathbb{R}^{m \times m}$, $1 < \ell < L$, and $W_1^L \in \mathbb{R}^{\sigma \times m}$. The notation $\Psi(x_t) = \max(0, x_t)$ refers to the ReLU activation function. We use a multi-layer perceptron as an example, but we will see in the experiments that f_1 can instantiate other neural architectures.

The network f_1 is trained by performing stochastic gradient descent with the mean squared error \mathcal{L}_1 between the predictions of f_1 and the observed feedback symbols, defined as

$$\mathcal{L}_1(\theta_1) = \sum_{\tau=1, h_\tau \in \Sigma_{\mathcal{I}}}^{t-1} \frac{(f_1(x_\tau, \theta_1) - e(h_\tau))^2}{2},$$

where $e(\cdot)$ refers to a σ -dimensional one-hot encoding. Note that θ_1 is updated based on the history of valid feedback symbols ($h_t \in \Sigma_{\mathcal{I}}$) and their associated observations (x_t).

Based on remark 4.7, the set of feedback distribution estimates over all the N actions in the game is defined as

$$\hat{\pi}(x_t) = \{\hat{\pi}_i(x) \text{ if } i \in \mathcal{I}, [1] \text{ otherwise}, i \in \{1, \dots, N\}\},$$

where $[1]$ is the feedback distribution vector of uninformative actions and $|\hat{\pi}(x)| = N$. The i -th element of $\hat{\pi}(x)$ is the feedback distribution estimate of action i . In Sec. 4.3, we will describe how $\hat{\pi}(x)$ is used to trade-off between exploration and exploitation.

Exploration network The exploration network f_2 estimates the prediction error of network f_1 . These estimates are used to quantify the uncertainty on the predictions of f_1 , and they are used to compute the confidence formula defined in Eq. 4.

Definition 4.8 (End-to-end embedding, Ban et al. [2024]). Given the exploitation network f_1 and an observation x_t , the end-to-end embedding is defined as

$$\phi(x_t) = \left[\Psi(W_1^1 x_t)^\top, \text{vec}(\nabla_{W_1^L} f_1(x_t, \theta_1)^\top) \right] \in \mathbb{R}^{m+\sigma m},$$

where the first element is the output vector of the first layer of f_1 and the second element is the flattened (represented by operator vec) partial derivative of f_1 with respect to the parameters of the last layer. In practice, $\phi(x_t)$ is normalized by dividing all the elements by the l_2 -norm of the vector.

To produce uncertainty estimates, the network f_2 learns the function $\Pi(x_t) - f_1(x_t, \theta_1)$. The network f_2 is instantiated as a multi-layer perceptron of depth L and width m , which receives the end-to-end embedding $\phi(x_t)$:

$$f_2(x_t, \theta_2) = W_2^L \Psi(W_2^{L-1} \Psi(W_2^{L-2} \dots \Psi(W_2^1 \phi(x_t)))),$$

where $W_2^1 \in \mathbb{R}^{m \times (m+\sigma m)}$, $W_2^\ell \in \mathbb{R}^{m \times m}$, $1 < \ell < L$, and $W_2^L \in \mathbb{R}^{\sigma \times m}$. The weights θ_2 of network f_2 are updated with stochastic gradient descent using the loss

$$\mathcal{L}_2(\theta_2) = \sum_{\tau=1, h_\tau \in \Sigma_{\mathcal{I}}}^{t-1} \frac{(f_2(x_\tau, \theta_2) - (e(h_\tau) - f_1(x_\tau, \theta_1)))^2}{2}.$$

Remark 4.9. The network f_2 is also based on the flattened vector representation of $\Pi(x_t)$. Therefore, the predictions of f_2 are σ -dimensional vectors. Since the number of symbols σ_i is known for any action by definition of the PM game, we can convert the flattened prediction vector of f_2 into a set of vectors.

Given remark 4.9, let $w(x_t) = \{\max(\hat{w}_i(x_t)) \text{ if } i \in \mathcal{I}, 0 \text{ otherwise}, i \in \{1, \dots, N\}\}$ denote the set of uncertainty estimates over all actions, where $|w(x_t)| = N$ and the notation $w_i(x_t)$ refers to the i -th element of $w(x_t)$. In other words, the uncertainty of an informative action corresponds to the maximum uncertainty value predicted by f_2 over the σ_i symbols induced by action i , denoted $\max(\hat{w}_i(x_t))$. This can be thought of as the worst-case uncertainty for the informative action i . For uninformative actions, the uncertainty is 0 following the heuristic that $\pi_i(x_t) = [1]$ for $i \notin \mathcal{I}$.

4.3 EXPLORATION AND EXPLOITATION

By leveraging the PM-extended EENets mechanism, NeuralCBP can compute $\hat{\delta}_{i,j}(x_t)$ for all neighbor action pairs $\{i, j\} \in \mathcal{N}$ using the feedback distributions predicted by network f_1 (see Eq. 3). It can also compute uncertainty estimates $z_{i,j}(x_t)$ on $\hat{\delta}_{i,j}(x_t)$ using the uncertainties predicted by network f_2 (see Eq. 4).

Following the CBP methodology, NeuralCBP then separates low uncertainty from high uncertainty estimates of $\hat{\delta}_{i,j}(x_t)$ by using a *successive elimination* [Even-Dar et al., 2002] criteria $|\hat{\delta}_{i,j}(x_t)| > z_{i,j}(x_t)$ for each action pair $\{i, j\} \in \mathcal{N}$. At round t , the pairs that verify the criteria are gathered in the set of confident pairs, denoted $\mathcal{U}(t)$. NeuralCBP leverages $\mathcal{U}(t)$ to compute a sub-space of the probability simplex Δ_M , defined as $D(t) = \{p \in \Delta_M, \{i, j\} \in \mathcal{U}(t), \text{sign}(\hat{\delta}_{i,j}(x_t))(\mathbf{c}_i - \mathbf{c}_j)p > 0\}$. The set $D(t)$ thus contains all likely outcome distributions given the confident

estimates of loss differences. The true (unknown) outcome distribution $p(x_t)$ is included with high confidence in the sub-space $D(t)$.

NeuralCBP then considers the set of *likely Pareto-optimal actions* $\mathcal{P}(t) \subseteq \mathcal{P}$ containing all Pareto-optimal actions $i \in \mathcal{P}$ such that their cell \mathcal{O}_i intersects with the sub-space $D(t)$. Similarly, it considers the set of *likely neighbors* $\mathcal{N}(t) \subseteq \mathcal{N}$ containing all neighbor action pairs $\{i, j\} \in \mathcal{N}$ such that their common cell $\mathcal{O}_i \cap \mathcal{O}_j$ intersects with $D(t)$. When $\mathcal{P}(t)$ contains only one action, $\mathcal{N}(t)$ is automatically empty, and therefore NeuralCBP exploits. When $\mathcal{P}(t)$ contains more than one action, it explores.

The selected action at round t . Let $X_{i,t} = \{\phi(x_\tau)\}_{\tau=1, i_\tau=i}^{t-1}$ denote the history up to time t (exclusively) of the observations embeddings under which action i was selected, and let $G_{i,t} = \lambda I_d + X_{i,t} X_{i,t}^\top$ denote the associated Gram matrix. Let the notation $\|x\|_S^2 = x^\top S x$ denote the norm of vector x weighted by some matrix S .

Definition 4.10 (Underplayed actions, Heuillet et al. [2024]). The set of underplayed actions, $\mathcal{R}(x_t) = \{i \in \{1, \dots, N\} \text{ s.t. } 1/\|x_t\|_{G_{i,t}^{-1}}^2 < \eta_i f(t)\}$, contains actions that have been played less than some play rate function $f(t)$ weighted by a scalar $\eta_i > 0$. The quantity $1/\|x_t\|_{G_{i,t}^{-1}}^2$ is a pseudo-count of the number of times action i was selected, weighted by the similarity between the current observation x_t and the observations at previous selections of action i .

Definition 4.11 (Neighborhood action set Bartók et al. [2012b]). The neighborhood action set of a neighbor pair $\{i, j\}$ is defined as $N_{i,j}^+ = \{k \in \{1, \dots, N\}, \mathcal{O}_i \cap \mathcal{O}_j \subseteq \mathcal{O}_k\}$. Note that $N_{i,j}^+$ naturally contains i and j . If $N_{i,j}^+$ contains another action k , then $\mathcal{O}_k = \mathcal{O}_i$ or $\mathcal{O}_k = \mathcal{O}_j$ or $\mathcal{O}_k = \mathcal{O}_i \cap \mathcal{O}_j$.

NeuralCBP computes the *likely neighbor* action set $\mathcal{N}^+(t) = \bigcup_{\{i,j\} \in \mathcal{N}(t)} N_{i,j}^+$ based on the remaining action pairs (likely neighbors) in $\mathcal{N}(t)$. Similarly, the set of *likely observer actions* is defined as $\mathcal{V}(t) = \bigcup_{\{i,j\} \in \mathcal{N}(t)} \mathcal{V}_{i,j}$.

The final set of actions considered by NeuralCBP at round t , denoted $\mathcal{S}(t)$, contains all potentially optimal actions (i.e. $\mathcal{P}(t) \cup \mathcal{N}^+(t)$) and all informative actions (i.e. $\mathcal{V}(t) \cup \mathcal{R}(x_t)$). From $\mathcal{S}(t)$, NeuralCBP selects the action with the greatest uncertainty weighted by $W_a = \max_{\{i,j\} \in \mathcal{N}} \|v_{ija}\|_\infty$, i.e. $a_t = \operatorname{argmax}_{i \in \mathcal{S}(t)} W_a w_a(x_t)$.

5 EXPERIMENTS

We compare the empirical performance of NeuralCBP to state-of-the-art baselines on a set of binary, multi-class, and cost-sensitive OAL classification tasks. To evaluate the robustness across neural architectures, we conduct experiments with a multi-layer perceptron (MLP) and the convolu-

tional architecture LeNet LeCun et al. [1998]. To our knowledge, our experiments are the first to evaluate OAL with a convolutional architecture. For reproducibility, we open-source the code base of NeuralCBP and the baselines. We also open-source the code base of PM-based OAL game environments. The code base is available on Github: <https://github.com/MaxHeuillet/neuralCBPside>.

Datasets For binary OAL tasks, we evaluate on **Adult** [Asuncion et al., 2007], **MagicTelescope** [Asuncion et al., 2007], and the **modified MNIST** [LeCun et al., 2010] (odds vs. even numbers) datasets. For multiclass OAL tasks, we consider **coverttype** and **shuttle** from the UCI repository [Asuncion et al., 2007], **MNIST** [LeCun et al., 2010], **Fashion** [Xiao et al., 2017], and **CIFAR10** [Krizhevsky et al., 2009]. For each dataset, we put aside 15% of the observations to create a separate fixed size *test set*, intended exclusively for evaluation of the generalization performance. We sample from the remaining observations a *deployment stream* that has a finite horizon of $T = 10k$ rounds. The OAL strategies acquire labelled data from the deployment stream. We run each experiment 25 times with different dataset splits for each run.

Baselines We compare NeuralCBP to six baselines. In the binary setting, we adapt the strategies Cesa and Margin, originally proposed for linear classifiers, to function with MLPs. We evaluate the multi-class state-of-the-art strategies INeural and Neuronal. Both INeural and Neuronal rely on a hyper-parameter γ that influences the amount of exploration. We consider respectively two instances of each strategy: one with the hyper-parameter configuration specified in their official publications ($\gamma = 6$ for Neuronal and INeural) and one that we chose to induce less exploration ($\gamma = 3$ for Neuronal and INeural). We further discuss implementation details and hyper-parameters in Appendix C.

Performance metrics To characterize the performance on the deployment stream, we measure the *final cumulative regret* achieved at the end of the stream (Eq. 1), which has to be minimized. We also report the *win count*, i.e. the number of times a strategy achieves the lowest final regret at the end of the horizon across the 25 runs of each experiment. Lastly, we perform *one-sided Welch’s t-tests* to assess if NeuralCBP’s final regret distribution is significantly lower than the baselines.

To evaluate the generalization performance and account for possible data imbalance in the considered datasets, we measure the *weighted f1-score* on the test sets. We measure the weighted f1-score while considering different volumes of expert-labelled observations acquired on the deployment stream (10, 25, 50, 100, 150, 250, 300, 400, 500, 750, 1000, 2500, 5000, 7500, 9000). Fixing the number of labelled observations allows for a fair comparison between the strategies.



Figure 1: Performance on binary OAL with MLP.

Lastly, we report the *average number of expert verifications* consumed by each strategy. It is important to note that, unlike previous experimental protocols [Ban et al., 2024, 2022b, DeSalvo et al., 2021], we do not set a maximum expert query budget. This choice aims to illustrate how each strategy effectively adapts its label complexity to the learning task. This choice reflects the realistic scenario where the optimal expert budget is unknown prior to deployment (as it largely depends on the dataset and type of architecture).

5.1 BINARY CASE

Figure 1a reports the final regrets achieved on the deployment stream. Numerical details are reported in Table 2 of Appendix C.1. `NeuralCBP` achieves the best final regret on the `MNISTbinary` and `Adult` datasets. On the `MagicTelescope` dataset, `NeuralCBP` achieves a final regret comparable `Neuronal`, `Cesa` and `Margin`, suggesting all these strategies are close to the optimal solution on this dataset. We observe that the final regret of all the strategies is subject to high variance (see Fig. 1a) caused by variations in the task difficulty over the 25 dataset splits. As a result, it is insightful to assess the performance solely based on the average final regret metric. The win count reveals that over 25 trials, `NeuralCBP` outperforms the baselines with 10

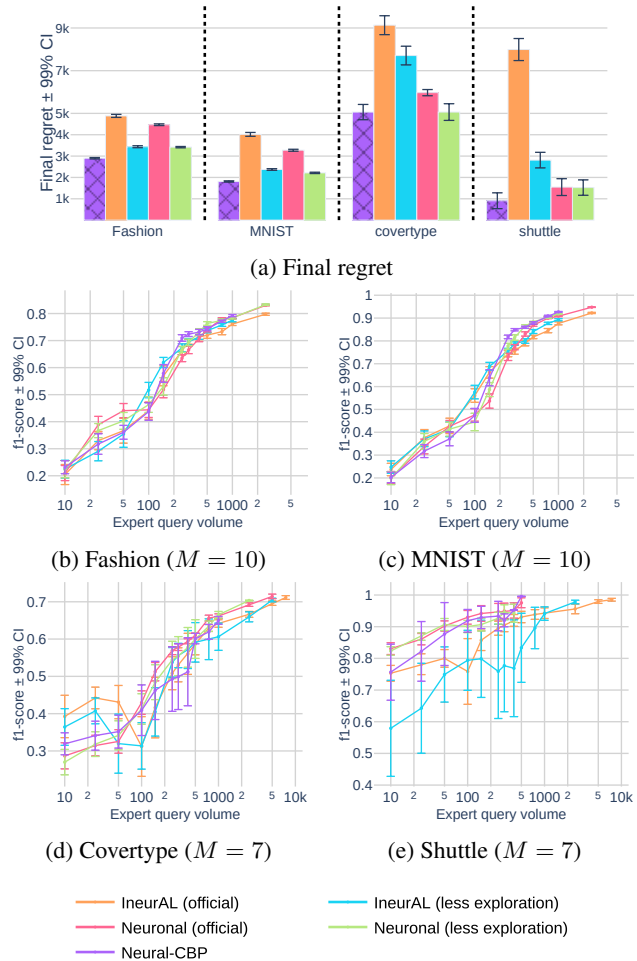


Figure 2: Performance on multi-class OAL with MLP.

wins on `MNISTbinary`, 14 wins on `MagicTelescope`, and 10 wins on `Adult`.

Figures 1b, 1c, and 1d display the weighted f1-score performance on the test sets for different volumes of expert queries. For each strategy, the f1-score curve stops at different expert-query volumes, which illustrates the *label complexity* of each approach. `NeuralCBP` exhibits a lower label query complexity (see Figures 1b and 1c) and achieves a f1-score performance that is comparable to the one achieved by the other baselines.

5.2 MULTI-CLASS CASE

Figure 2a reports the final regret on multi-class tasks. Numerical values are reported in Table 4 (Appendix C.1). `NeuralCBP` consistently achieves the lowest final regret on the four datasets considered. The improvement in final regret performance is statistically significant for `MNIST`, `Fashion` and `adult` datasets (all p-values < 0.01), and `NeuralCBP` achieves identical performance to `Neuronal (less exploration)` on `covertype`. The improvement ranges from 15% to 40% over the second best baseline (`Neuronal with less exploration`) on `MNIST`, `Fashion`, and `shuttle` datasets.

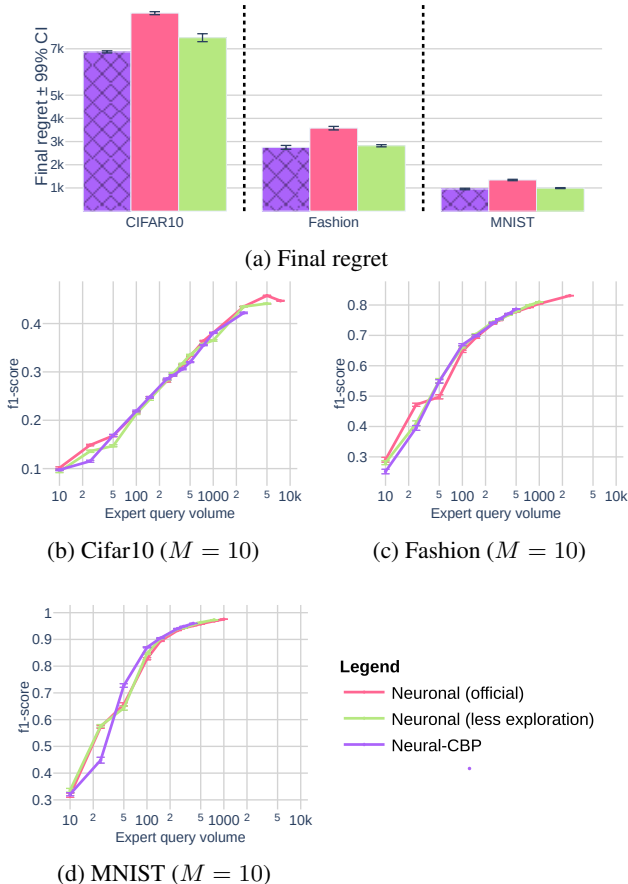


Figure 3: Performance on multi-class OAL with LeNet.

Figures 2b, 2c, 2d and 2e show that given the same volume of expert queries, *NeuralCBP* achieves a comparable or better f_1 -score performance on the test sets. Other strategies may achieve a f_1 -score performance increase at the expense of significantly more expert queries. However, the generalization improvement obtained from these additional labelled observations is not reflected in terms of final regret performance.

Robustness across different neural architectures. We now evaluate *Neuronal* and *NeuralCBP* on a set of multi-class tasks using the convolutional architecture LeNet [LeCun et al., 1998]. *INeural* is omitted because it requires one-hot encodings of observations in the action space, which is not scalable when operating over multi-dimensional tensor observations. See numeric details in Table 6.

Figure 3a shows that *NeuralCBP* achieves the best final regret performance. Furthermore, *NeuralCBP* achieves a comparable f_1 -score performance compared to *Neuronal* for equivalent volumes of expert queries. While the f_1 -score curves show little difference between *NeuralCBP* and *Neuronal*, it is worth noting that *NeuralCBP* has a smaller label complexity. Indeed, the additional exploration performance by *Neuronal* (official) and *Neuronal* (less

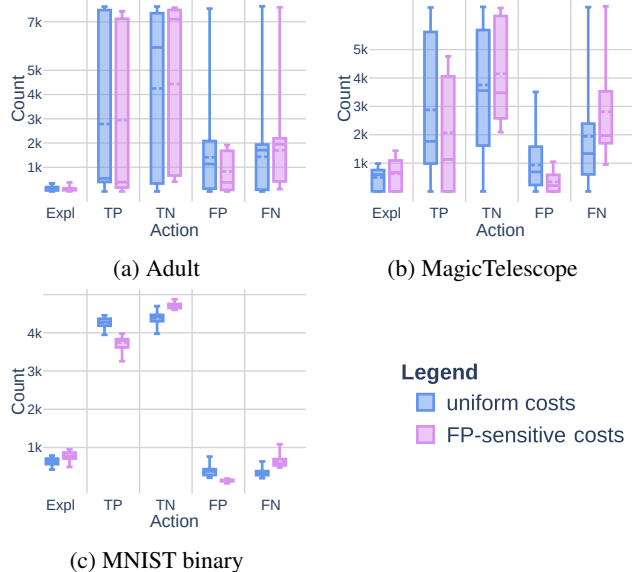


Figure 4: Distribution of the number of expert queries (Expl), true positives (TP), true negatives (TN), false positives (FP), and false negatives (FN) for *NeuralCBP* playing Label-efficient with uniform cost vs high cost on FP. Intrinsic goal of FP-sensitive: Minimize the count of FP.

exploration) is not reflected into a better final regret performance.

5.3 SPECIFYING A COST STRUCTURE

In this experiment, we investigate the impact of cost-sensitivity on the action selection strategy of *NeuralCBP*. To our knowledge, *NeuralCBP* is the only applicable strategy in cost-sensitive OAL tasks. We consider the previous binary OAL tasks conducted on *Adult*, *MagicTelescope*, and the modified *MNIST* datasets.

Recall from Section 3 that the original label efficient game corresponds to a binary classification task where the costs of prediction errors and expert queries are equal to 1 across the two classes. We refer to this formulation as the **uniform costs** case. We also consider a cost-sensitive variation where the cost of false negatives (FN) is twice as low as the cost of false positives (FP). We refer to this cost-sensitive variation as the **FP-sensitive costs** case. In the FP-sensitive case, the intrinsic goal is to minimize the amount of false positives. For example, this could refer to a learning system constrained to minimize incorrect positive detection in medical screenings (HIV, cancer, etc).

Figure 4 illustrates the influence of the cost structure on *NeuralCBP*. We measure the count distribution (mean, median, 1st and 3rd quartiles) of expert queries, true positives (TP), true negatives (TN), false positives (FP), and false negatives (FN), over the 25 runs. In *Adult* and *MagicTe*

lescope datasets (Figures 4a and 4b), the third quartile of the FP count is approximately 3 times smaller under the FP-sensitive cost structure. On MNIST binary (Figure 4c), the mean FP count is 336 ± 112.24 (1-std) in the uniform case; this value drops to 136 ± 30 (1-std) in the FP-sensitive case. These numeric results show that `NeuralCBP` successfully accounts for the specified FP-sensitive cost structure.

6 DISCUSSION

General feedback structure. `NeuralCBP` is a strategy designed for the partial monitoring setting. To account for partial monitoring games, `NeuralCBP` operates a distinction between incurred costs (not learned, specified in the cost matrix \mathbf{C}), observable feedbacks (not learned, specified in the feedback matrix \mathbf{H}) and feedback distribution (learned components noted $\hat{\pi}_a(x_t)$ for each action a). This formulation brings an answer to Ban et al. [2024] who were the first to question the optimality of bandit feedback structure in OAL. On the practical side, `NeuralCBP` enables to specify a cost structure and partial monitoring games capture the presence of multiple experts.

Distinct exploration principles. In existing `EENets` strategies, the predictions of the network f_2 are added to the predictions of f_1 to compute an *upper confidence bound* on the predictions. Then, the magnitude of the difference between the top two predictions drives the exploration. In contrast, the predictions of network f_2 in `NeuralCBP` contribute to a *successive elimination* criteria (defined in Section 4.3) that checks whether the upper and lower confidence bounds of two different actions overlaps or not.

Sensitivity to hyper-parameters In `Neuronal` and `INeural` strategies, the decision of querying the expert is based on the difference between the top two class predictions. If the difference is greater than a slack term (obtained from the theory), the strategy asks for an expert label. The slack term provided by the theory is not usually computed in practice Ban et al. [2024]. Therefore, the user must select a proxy γ of the slack term. As demonstrated in our experiments, we have evaluated the official ($\gamma = 0.6$) instances of `Neuronal` and `INeural`, as well as instances that induce less exploration ($\gamma = 3$). We observe from Figures 1, 2, 3, 5, 6 and 7 that the final regret performance of `Neuronal` and `INeural` on a specific stream of observations is sensitive to an appropriate choice of γ . One benefit of `NeuralCBP` over `Neuronal` and `INeural` is that the exploration is driven by a successive elimination criteria that is hyper-parameter free. This algorithmic characteristic is relevant in the context of online learning, where deployment data is unknown in advance, making it difficult to appropriately tune hyper-parameters.

7 CONCLUSION

Our work advocates for the adoption of the partial monitoring framework in practice, a field traditionally supported by theoretical research. We leverage the PM framework to formulate OAL tasks and propose `NeuralCBP`, the first PM strategy able to learn efficiently from neural networks. While the emphasis of this paper is on OAL, `NeuralCBP` is a general PM approach that can be applied to the broader diversity of partial monitoring games. We demonstrate the empirical performance of `NeuralCBP` on a set of binary, multi-class and cost-sensitive OAL tasks, and highlight technical and empirical benefits over existing OAL strategies.

Limitations A limitation of `NeuralCBP` is that it does not scale well with large number of classes. Combinatorial PM strategies could address this limitation [Lin et al., 2014]. Furthermore, `NeuralCBP` does not capture the multi-expert case. The multi-expert case is studied in Dekel et al. [2012], Kumar et al. [2022] without the PM framework but a PM perspective based on Kirschner et al. [2020, 2023] could be an avenue of future research.

Author Contributions

Maxime Heuillet: conceptualization, methodology, empirical investigation, visualizations, implementation, writing (original draft, editing), funding acquisition. Ola Ahmad: conceptualization, writing (review, editing), supervision. Audrey Durand: conceptualization, writing (review, editing), supervision, funding acquisition.

Acknowledgements

This work was funded through a Mitacs Accelerate grant. We thank Alliance Canada and Calcul Quebec for access to computational resources and staff expertise consultation. We would like to thank Dr. Yikun Ban for answering our technical questions about `INeural` and `Neuronal`.

References

- Kareem Amin, Corinna Cortes, Giulia DeSalvo, and Afshin Rostamizadeh. Understanding the effects of batching in online active learning. In *In Proc. AISTATS*, 2020.
- Arthur Asuncion et al. Uci machine learning repository, 2007.
- Maria-Florina Balcan, Andrei Broder, and Tong Zhang. Margin based active learning. In *In Proc. COLT*, pages 35–50, 2007.
- Yikun Ban, Yuchen Yan, Arindam Banerjee, and Jingrui He. Ee-net: Exploitation-exploration neural networks in contextual bandits. In *proc. ICLR*, 2022a.

- Yikun Ban, Ishika Agarwal, Ziwei Wu, Yada Zhu, Kommy Weldemariam, Hanghang Tong, and Jingrui He. Neural active learning beyond bandits. In *The Twelfth International Conference on Learning Representations*, 2024.
- Yikun Ban et al. Improved algorithms for neural active learning. In *Proc. NeurIPS*, 2022b.
- Gábor Bartók et al. Partial monitoring with side information. In *In Proc. ALT*, 2012a.
- Gábor Bartók et al. An adaptive algorithm for finite stochastic partial monitoring. In *Proc. ICML*, 2012b.
- Gábor Bartók et al. Partial monitoring - classification, regret bounds, and algorithms. *Mathematics of Operations Research*, 39(4):967–997, 2014.
- Alina Beygelzimer, Sanjoy Dasgupta, and John Langford. Importance weighted active learning. In *In Proc. ICML*, pages 49–56, 2009.
- Ting Cai et al. Active cost-aware labeling of streaming data. In *In Proc. AISTATS*, 2023.
- Nicoló Cesa-Bianchi, Claudio Gentile, and Luca Zaniboni. Worst-case analysis of selective sampling for linear classification. *JMLR*, 7(44):1205–1230, 2006.
- David Cohn, Les Atlas, and Richard Ladner. Improving generalization with active learning. *Machine learning*, 15:201–221, 1994.
- Ofer Dekel, Claudio Gentile, and Karthik Sridharan. Selective sampling and active learning from single and multiple teachers. *The Journal of Machine Learning Research*, 13(1):2655–2697, 2012.
- Giulia DeSalvo et al. Online active learning with surrogate loss functions. In *Proc. NeurIPS*, 2021.
- Charles Elkan. The foundations of cost-sensitive learning. In *In Proc. IJCAI*, volume 17, pages 973–978. Lawrence Erlbaum Associates Ltd, 2001.
- Eyal Even-Dar, Shie Mannor, and Yishay Mansour. Pac bounds for multi-armed bandit and markov decision processes. In *COLT*, volume 2, pages 255–270. Springer, 2002.
- David Helmbold et al. Some label efficient learning results. In *In Proc. CoLT*, 1997.
- Maxime Heuillet et al. Randomized confidence bounds for stochastic partial monitoring, 2024.
- Johannes Kirschner, Tor Lattimore, and Andreas Krause. Linear partial monitoring for sequential decision-making: Algorithms, regret bounds and applications. *JMLR*, 2023.
- Johannes Kirschner et al. Information directed sampling for linear partial monitoring. *PMLR*, 2020.
- Alex Krizhevsky, Geoffrey Hinton, et al. Learning multiple layers of features from tiny images. 2009.
- Bhuvesh Kumar et al. ActiveHedge: Hedge meets active learning. In Kamalika Chaudhuri, Stefanie Jegelka, Le Song, Csaba Szepesvari, Gang Niu, and Sivan Sabato, editors, *In proc. ICML*, volume 162, pages 11694–11709, 2022.
- A Gilad Kusne, Heshan Yu, Changming Wu, Huairuo Zhang, Jason Hattrick-Simpers, Brian DeCost, Suchismita Sarker, Corey Oses, Cormac Toher, Stefano Curtarolo, et al. On-the-fly closed-loop materials discovery via bayesian active learning. *Nature communications*, 11(1):5966, 2020.
- Y. LeCun, C. Cortes, and C. J. C. Burges. The mnist database of handwritten digits. <http://yann.lecun.com/exdb/mnist/>, 2010.
- Yann LeCun, Léon Bottou, Yoshua Bengio, and Patrick Haffner. Gradient-based learning applied to document recognition. *Proceedings of the IEEE*, 86(11):2278–2324, 1998.
- Ian Lienert. Exploiting side information in partial monitoring games: An empirical study of the cbp-side algorithm with applications to procurement. Master’s thesis, Eidgenössische Technische Hochschule Zürich, Department of Computer Science, 2013.
- Tian Lin, Bruno Abrahao, Robert Kleinberg, John Lui, and Wei Chen. Combinatorial partial monitoring game with linear feedback and its applications. In *In Proc. ICML*, pages 901–909. PMLR, 2014.
- Antonio Piccolboni et al. Discrete prediction games with arbitrary feedback and loss. In *Proc. CoLT*, 2001.
- Akanksha Saran, Safoora Yousefi, Akshay Krishnamurthy, John Langford, and Jordan T Ash. Streaming active learning with deep neural networks. *arXiv preprint arXiv:2303.02535*, 2023.
- David Sculley. Practical learning from one-sided feedback. In *Proceedings of the 13th ACM SIGKDD international conference on Knowledge discovery and data mining*, pages 609–618, 2007.
- Jack Sherman et al. Adjustment of an Inverse Matrix Corresponding to a Change in One Element of a Given Matrix. *The Annals of Mathematical Statistics*, 21(1):124 – 127, 1950.
- Adish Singla et al. Contextual procurement in online crowdsourcing markets. In *In Proc. AAAI*, 2014.
- Dirk van der Hoeven, Federico Fusco, and Nicolò Cesa-Bianchi. Beyond bandit feedback in online multiclass classification. In *Proc. NeurIPS*, 34:13280–13291, 2021.

Zhilei Wang et al. Neural active learning with performance guarantees. *In Proc. NeurIPS*, 2021.

Han Xiao, Kashif Rasul, and Roland Vollgraf. Fashion-mnist: a novel image dataset for benchmarking machine learning algorithms. *arXiv preprint arXiv:1708.07747*, 2017.

Pan Xu, Zheng Wen, Handong Zhao, and Quanquan Gu. Neural contextual bandits with deep representation and shallow exploration. In *In Proc. ICLR*, 2022.

Neural Active Learning Meets the Partial Monitoring Framework (Supplementary Material)

Maxime Heuillet¹

Ola Ahmad^{1,3}

Audrey Durand^{1,2}

¹Université Laval, Canada

²Canada-CIFAR AI Chair, Mila, Canada

³Thales Research and Technology (cortAIX), Canada,

Notation	Definition	Observable by the agent?
N	Number of actions	✓
M	Number of outcomes	✓
E	Number of experts	✓
Σ	Feedback space (space of symbols)	✓
$\mathbf{C} \in [0, 1]^{N \times M}$	Cost matrix	✓
\mathbf{c}_i	Row i in matrix \mathbf{C} (associated with action i)	✓
$\mathbf{H} \in \Sigma^{N \times M}$	Feedback matrix	✓
\mathbf{h}_i	Row i in matrix \mathbf{H} (associated with action i)	✓
σ_i	Number of unique feedback symbols induced by action i (i.e. on row i of H)	✓
Δ_M	Probability simplex of dimension M (i.e. over the outcome space)	✓
Δ_{σ_i}	Probability simplex of dimension σ_i (i.e. over the symbol space induced by action i)	✓
T	Total number of rounds in a game (horizon)	✗
i_t	Action played by the agent at round t	✓
y_t	Outcome at round t	✗
h_t	Feedback symbol at round t	✓
$\mathbf{H}[i_t, y_t]$	Element in matrix \mathbf{H} at row I_t and column J_t (i.e. feedback received at round t)	✓
$\mathbf{C}[i_t, y_t]$	Element in matrix \mathbf{C} at row I_t and column J_t (i.e. loss incurred at round t)	✗
\mathcal{X}	Observation space	✗
\mathcal{I}	Set of informative actions	✓
$\Sigma_{\mathcal{I}}$	Valid feedback symbols	✓
$\Pi(x_t)$	Set of informative feedback distributions	✗
$x_t \in \mathcal{X}$	Observation received at time t	✓
$X_{i,t}$	History of end-to-end embeddings for action i up to time t	✓
$G_{i,t}$	Gram matrix for action i up to time t	✓
$p(x_t) \in \Delta_M$	Outcome distribution	✗
$\mathcal{O}_i \subseteq \Delta_M$	Cell of action i	✓
Σ_i	Enumeration of symbols sorted by order of appearance in h_i	✓
$S_i \in \{0, 1\}^{\sigma_i \times M}$	Signal matrix of action i	✓
$\pi_i(x_t) \in \Delta_{\sigma_i}$	Distribution for the unique feedback symbols induced by action i	✗
$\delta_{i,j}(x_t)$	Expected loss difference between action i and j	✗
\mathcal{P}	Set of Pareto optimal actions (i.e. set of actions)	✓
\mathcal{N}	Set of neighbor action pairs (i.e. set of pairs of actions)	✓
$\mathcal{U}(t)$	Set of confident action pairs (i.e. set of pairs of actions)	✓
$V_{i,j}$	Observer set for pair i, j (i.e. set of actions)	✓
v_{ija}	Observer vector associated with $V_{i,j}$ (index a indicates to which action in $V_{i,j}$ it is associated to)	✓
$z_{i,j}(t)$	Confidence for a pair $\{i, j\}$ at round t	✓
$D(t) \subseteq \Delta_M$	Sub-space of the simplex based on constraints in $\mathcal{U}(t)$, it includes p^* with high confidence	✓
$\mathcal{N}_{i,j}^+$	Neighbor action set for pair i, j (set of actions)	✓
$\mathcal{P}(t)$	Plausible subset of \mathcal{P} given $D(t)$ (set of actions)	✓
$\mathcal{N}(t)$	Plausible subset of \mathcal{N} given $D(t)$ (set of pairs of actions)	✓
$\mathcal{R}(x_t)$	Set of underplayed actions at time t (set of actions)	✓
$e(\cdot)$	One hot encoding	✓
$\mathcal{S}(t)$	Final set of actions considered by CBP (set of actions)	✓
$W_a = \max_{\{i,j\} \in \mathcal{N}} \ v_{ija}\ _{\infty}$	Weight of an action	✓

Table 1: List of notations

A ANALYSIS OF THE LABEL EFFICIENT GAME

The original label-efficient game [Helmbold et al., 1997] is defined by the following cost and feedback matrices:

$$\mathbf{C} = \begin{array}{c} \text{pred. class A} \\ \text{pred. class B} \\ \text{expert} \end{array} \begin{array}{cc} \text{class A} & \text{class B} \\ \left[\begin{array}{cc} 0 & 1 \\ 1 & 0 \\ 1 & 1 \end{array} \right] \end{array}, \mathbf{H} = \begin{array}{cc} \text{class A} & \text{class B} \\ \left[\begin{array}{cc} \diamond & \diamond \\ \wedge & \wedge \\ \perp & \odot \end{array} \right] \end{array}.$$

The game includes a set of $N = 3$ possible actions and $M = 2$ possible outcomes (class A, and class B). For actions 1 and 2, there is $\sigma_1 = \sigma_2 = 1$ unique feedback symbol. For action 3, there is $\sigma_3 = 2$ feedback symbols, and the enumeration is $\{\perp, \odot\}$. Therefore, the set of informative actions is $\mathcal{I} = \{3\}$.

Signal Matrices: The dimension of the signal matrices are such that $S_1 \in \{0, 1\}^{1 \times 2}$ and $S_2 \in \{0, 1\}^{1 \times 2}$ and $S_3 \in \{0, 1\}^{2 \times 2}$. The matrices verify:

$$S_1 = [1 \quad 1], \quad S_2 = [1 \quad 1], \quad S_3 = \begin{bmatrix} 1 & 0 \\ 0 & 1 \end{bmatrix}$$

The outcome distribution is noted $p^* = [p_A, p_B]^\top$.

Cells: Each action can be associated to a sub-space of the probability simplex noted *cell* (see Definition 2.1):

- For action 1, we have: $\mathcal{O}_1 = \{p \in \Delta_M, \forall j \in \{1, \dots, N\}, (\mathbf{c}_1 - \mathbf{c}_j)p \leq 0\}$. This probability space corresponds to the following constraints:

$$\begin{bmatrix} \mathbf{c}_1 - \mathbf{c}_1 \\ \mathbf{c}_1 - \mathbf{c}_2 \\ \mathbf{c}_1 - \mathbf{c}_3 \end{bmatrix} p = \begin{bmatrix} 0 & 0 \\ -1 & 1 \\ -1 & 0 \end{bmatrix} p \leq 0$$

The first constraint $(\mathbf{c}_1 - \mathbf{c}_1)p \leq 0$ is always verified. The second constraint $(\mathbf{c}_1 - \mathbf{c}_2)p \leq 0$ implies $-p_A + p_B \leq 0 \iff p_B \leq p_A$. The third constraint $(\mathbf{c}_1 - \mathbf{c}_3)p \leq 0$ implies $-p_A \leq 0 \iff p_A \geq 0$.

- For action 2, we have: $\mathcal{O}_2 = \{p \in \Delta_M, \forall j \in \{1, \dots, N\}, (\mathbf{c}_2 - \mathbf{c}_j)p \leq 0\}$. This probability space corresponds to the following constraints:

$$\begin{bmatrix} \mathbf{c}_2 - \mathbf{c}_1 \\ \mathbf{c}_2 - \mathbf{c}_2 \\ \mathbf{c}_2 - \mathbf{c}_3 \end{bmatrix} p = \begin{bmatrix} 1 & -1 \\ 0 & 0 \\ 0 & -1 \end{bmatrix} p \leq 0$$

The second constraint $(\mathbf{c}_2 - \mathbf{c}_2)p \leq 0$ is always satisfied. The first constraint $(\mathbf{c}_2 - \mathbf{c}_1)p \leq 0$ implies $p_A - p_B \leq 0 \iff p_A \leq p_B$. The third constraint $(\mathbf{c}_2 - \mathbf{c}_3)p \leq 0$ implies $-p_B \leq 0 \iff p_B \geq 0$.

- For action 3, we have: $\mathcal{O}_3 = \{p \in \Delta_M, \forall j \in \{1, \dots, N\}, (\mathbf{c}_3 - \mathbf{c}_j)p \leq 0\}$. This probability space corresponds to the following constraints:

$$\begin{bmatrix} \mathbf{c}_3 - \mathbf{c}_1 \\ \mathbf{c}_3 - \mathbf{c}_2 \\ \mathbf{c}_3 - \mathbf{c}_3 \end{bmatrix} p = \begin{bmatrix} 1 & 0 \\ 0 & 1 \\ 0 & 0 \end{bmatrix} p \leq 0$$

The third constraint $(\mathbf{c}_3 - \mathbf{c}_3)p \leq 0$ is always verified. The first constraint $(\mathbf{c}_3 - \mathbf{c}_1)p \leq 0$ implies $p_A \leq 0$ and the second constraint $(\mathbf{c}_3 - \mathbf{c}_2)p \leq 0$ implies $p_B \leq 0$. There exist no probability vector in Δ_M satisfying these three constraints at the same time.

Pareto optimal actions: From the analysis of the cells, we have $\mathcal{O}_3 = \emptyset$. Therefore, action 3 is dominated, according to Definition 2.1. The remaining actions 1 and 2 are Pareto optimal because their respective cells are not included in one another, i.e. $\mathcal{P} = \{1, 2\}$.

Neighbor actions: In this paragraph, we will determine whether action 1 and 2 are a neighbor pair.

$$\mathcal{O}_1 \cap \mathcal{O}_2 = \begin{cases} p_B \leq p_A \\ p_A \geq 0 \\ p_A \leq p_B \\ p_B \geq 0 \end{cases}$$

The only point in this vector space is $[0.5 \ 0.5]^\top$. Therefore, $\dim(\mathcal{O}_1 \cap \mathcal{O}_2) = 0 = M - 2$ and the pair $\{1, 2\}$ is a neighbor pair, i.e. $\mathcal{N} = \{\{1, 2\}, \}$.

Neighbor action set: This set is defined as $N_{ij}^+ = \{k \in \{1, \dots, N\}, \mathcal{O}_i \cap \mathcal{O}_j \subset \mathcal{O}_k\}$. This yields: $N_{1,2}^+ = N_{2,1}^+ = [1, 2]$ because the cell of action 3 is empty.

Informative action set Action 3 is the only informative action because $\sigma_3 = 2 \geq 1$.

Observer set: We have: $V_{1,2} = \{3\}$ same applies to $V_{2,1} = \{3\}$, because action 3 is the only informative action.

Observer vector: For the pair $\{1, 2\}$, we have to find $v_{ija}, a \in V_{ij}$ such that $C_1^\top - C_2^\top = \sum_{a \in V_{ij}} S_i^T v_{ija}$, according to Definition 4.3. Choosing and $v_{121}^\top = [-1 \ 1]$ verifies the relation:

$$\mathbf{c}_1^\top - \mathbf{c}_2^\top = \begin{bmatrix} -1 \\ 1 \end{bmatrix} = \begin{bmatrix} 1 & 0 \\ 0 & 1 \end{bmatrix} \begin{bmatrix} -1 \\ 1 \end{bmatrix}$$

B IMPLEMENTATION DETAILS

The pseudo-code in Algorithm 2 details how the EENet s is updated.

Algorithm 2: Update EENet with gradient descent

input : θ_1, θ_2

1 Epoch number K_1 and K_2 , learning rate η_1 and η_2

2 Initialize $\theta_1^{(0)} = \theta_1$

3 **for** $k \in \{1, \dots, K_1\}$ **do**

4 $\theta_1^{(k)} = \theta_1^{(k-1)} - \mu_1 \nabla_{\theta_1^{(k-1)}} \mathcal{L}_1(\theta_1^{(k-1)})$;

5 $\tilde{\theta}_1 = \theta_1^{(K_1)}$

6 Initialize $\theta_2^{(0)} = \theta_2$

7 **for** $k \in \{1, \dots, K_2\}$ **do**

8 $\theta_2^{(k)} = \theta_2^{(k-1)} - \mu_2 \nabla_{\theta_2^{(k-1)}} \mathcal{L}_2(\theta_2^{(k-1)})$;

9 $\tilde{\theta}_2 = \theta_2^{(K_2)}$

output : $\tilde{\theta}_1, \tilde{\theta}_2$

C EXPERIMENT DETAILS.

The neural components of the strategies refer to two networks f_1 and f_2 for NeuralCBP, Neuronal and INeural; f_1 is trained using the MSE loss functions \mathcal{L}_1 and f_2 with \mathcal{L}_2 . For strategies Cesa and Margin, the neural component corresponds to one network f_1 , which is trained using the MSE loss function \mathcal{L}_1 . In the experiments with a MLP, f_1 is a MLP architecture of width $m = 100$ and depth $L = 2$, and f_2 is a MLP of width $m = 100$ and depth $L = 2$. In the experiments with a LeNet, f_1 is a LeNet architecture LeCun et al. [1998], and f_2 is a MLP of width $m = 100$ and depth $L = 2$.

Update protocol for the neural components of the strategies. At the beginning of the game, each strategy plays each action once. Then, to save compute, we perform updates at every round for the first $N \leq t \leq 50$ steps. We update every 50 rounds for $t \leq 1000$. Finally, we update every 500 rounds when $t \geq 1000$. An equivalent update protocol has been used in related neural online learning literature Xu et al. [2022]. This update protocol is implemented for all the strategies considered in the experiments.

End-to-end embedding down sampling. Both `Neuronal` and `NeuralCBP` use the *end-to-end embedding* (see Definition 4.8). Due to the dimension of a flattened gradient, the embedding received as input to f_2 requires a down-sampling. Similarly to Ban et al. [2024], we use a *block-reduction averaging operator*. When f_1 is based on a MLP architecture, the reduction parameter is 51 following Ban et al. [2024]. When f_1 is based on a LeNet architecture, we set the reduction parameter to 51 for MNIST and FASHION datasets. For CIFAR10, we increase the block averaging to $153 = 51 \times 3$ to account for the three color channels (RGB) of CIFAR10 observations.

NeuralCBP. To speed up compute, the inversion and updates of the Gram matrix are performed on GPU, using the Sherman-Morison update [Sherman et al., 1950]. We set $f(t) = \alpha^{1/3} t^{2/3} \log(t)^{1/3}$, $\eta_a = W_a^{2/3}$ and $\alpha = 1.01$ according to previous literature Heuillet et al. [2024]. This combination of parameters is justified by the theoretical analysis of CBP and is not meant to be tuned further.

To update f_1 and f_2 , we use the Adam optimizer, with the learning rate set to the default value $\mu_1 = \mu_2 = 0.001$ (both for MLP and LeNet architectures). Following Ban et al. [2024], we set the batch size to 64 and the number of epochs to 40. We performed a grid search for the learning rate over $\{0.0001, 0.001\}$ and found that the value 0.001 performs best.

Neuronal The strategy `Neuronal` admits a hyper-parameter γ that influences the amount of exploration. For `Neuronal` (official), we set $\gamma = 6$, as reported in Ban et al. [2024]. We also consider the instance $\gamma = 3$ for `Neuronal` (less exploration), which exhibits less exploration.

Following Ban et al. [2024], we set the batch size to 64 and the number of epochs to $K_1 = K_2 = 40$. For f_1 and f_2 , we use the Adam optimizer, with the value for the learning rate set at $\mu_1 = \mu_2 = 0.001$ for both the MLP, and LeNet architecture. We performed a grid search and report empirical findings for the learning rate over $\{0.0001, 0.001\}$. We observed from Tables 2, 3, 4, 5 and 6, 7 that a learning rate $\mu_1 = \mu_2 = 0.001$ performs best on most datasets for both instances of `Neuronal` (official and $\gamma = 3$).

INeural The exploration parameter is set to $\gamma = 6$ for `INeural` (official) and to $\gamma = 3$ for `INeural` (less exploration). Note that the networks f_1 and f_2 of `INeural` have a different input dimension, as they require input observations to be one-hot-encoded over the action space.

For f_1 and f_2 , we use the Adam optimizer, with the default value for the learning rate set at $\mu_1 = \mu_2 = 0.001$. The batch size is set to 64 and the number of epochs to 40. This approach is known to be outperformed by `Neuronal`, we used the set of optimal hyper-parameters reported in Ban et al. [2024].

Cesa The exploration strategy of the approach `Cesa` is hyper-parameter free. For the network f_1 , we use the Adam optimizer, with the default value for the learning rate set at $\mu_1 = 0.001$. The batch size is set to 64 and the number of epochs to $K_1 = 40$.

Margin The exploration parameter of the `Margin` approach is set to 1. For network f_1 , we use the Adam optimizer, with the default value for the learning rate set at $\mu_1 = 0.001$. The batch size is set to 64 and the number of epochs to $K_1 = 40$.

C.1 NUMERIC RESULTS

In this Appendix, we report the empirical performance of `Neuronal` with a learning rate set to $\mu_1 = \mu_2 = 0.0001$. We also report numeric details for all the figures reported in the main body and appendix.



Figure 5: Performance on binary OAL with MLP. Neuronal with $\mu_1 = \mu_2 = 0.0001$.

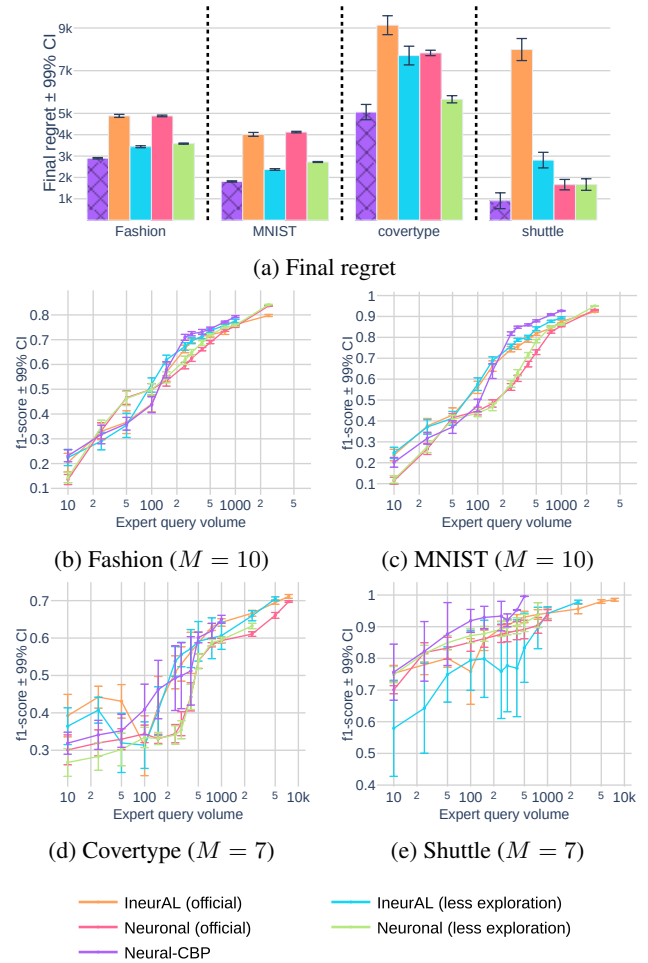


Figure 6: Performance on multi-class OAL with MLP. Neuronal with $\mu_1 = \mu_2 = 0.0001$.

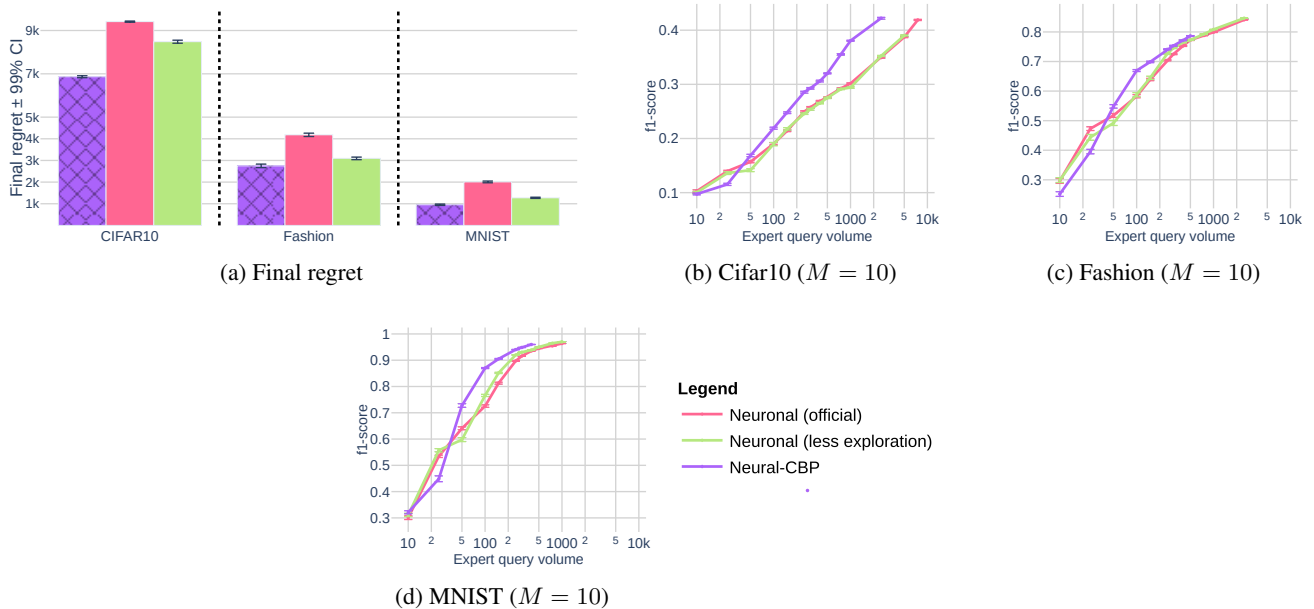


Figure 7: Performance on multi-class OAL with LeNet. Neuronal with $\mu_1 = \mu_2 = 0.0001$.

Dataset	Approach	Mean regret	p-value	win count	Mean Exploration	p-value (exploration)
MNIST binary	Neural-CBP	1351.92	1.0	10.0	638.32	1.0
MNIST binary	IneurAL (official)	1701.72	0.0	0.0	1311.44	0.0
MNIST binary	IneurAL (less exploration)	1701.28	0.103	2.0	624.96	0.756
MNIST binary	Neuronal (official)	1566.16	0.0	0.0	1363.88	0.0
MNIST binary	Neuronal (less exploration)	1646.16	0.172	13.0	778.4	0.01
MNIST binary	Cesa	2627.52	0.0	0.0	303.28	0.0
MNIST binary	Margin	3169.6	0.0	0.0	100.28	0.0
MagicTelescope	Neural-CBP	3370.36	1.0	14.0	496.68	1.0
MagicTelescope	IneurAL (official)	7343.04	0.0	0.0	6452.8	0.0
MagicTelescope	IneurAL (less exploration)	4473.2	0.0	0.0	3138.28	0.0
MagicTelescope	Neuronal (official)	3716.8	0.207	0.0	1604.84	0.0
MagicTelescope	Neuronal (less exploration)	3287.0	0.769	7.0	444.64	0.613
MagicTelescope	Cesa	3245.64	0.623	1.0	328.76	0.033
MagicTelescope	Margin	3574.12	0.483	3.0	58.04	0.0
adult	Neural-CBP	2968.88	1.0	10.0	127.64	1.0
adult	IneurAL (official)	8243.12	0.0	0.0	7610.2	0.0
adult	IneurAL (less exploration)	3909.48	0.027	0.0	1136.24	0.0
adult	Neuronal (official)	3222.24	0.551	1.0	951.72	0.025
adult	Neuronal (less exploration)	3035.92	0.884	5.0	89.64	0.379
adult	Cesa	3180.0	0.643	3.0	320.12	0.001
adult	Margin	3166.56	0.682	6.0	19.92	0.0

Table 2: Supplement for Section 5.1 presented in the main paper (see Figure 1). Neuronal with $\mu_1 = \mu_2 = 0.001$. Mean regret: average regret at the last step ($T = 10k$). P-value: Welch’s t-test on the distribution of regrets at the last step, with NeuralCBP as reference (p-value > 0.05 means no statistical difference). Win count: number of times a given strategy achieved the lowest final regret (ties included). Mean exploration: average number of expert-verified observations. P-value (exploration): Welch’s t-test on the distribution of number of expert queries.

Dataset	Approach	Mean regret	p-value	win count	Mean Exploration	p-value (exploration)
MNIST binary	Neural-CBP	1351.92	1.0	15.0	638.32	1.0
MNIST binary	IneurAL (official)	1701.72	0.0	0.0	1311.44	0.0
MNIST binary	IneurAL (less exploration)	1701.28	0.103	8.0	624.96	0.756
MNIST binary	Neuronal (official)	1730.08	0.0	0.0	1558.76	0.0
MNIST binary	Neuronal (less exploration)	1440.48	0.005	2.0	987.84	0.0
MNIST binary	Cesa	2627.52	0.0	0.0	303.28	0.0
MNIST binary	Margin	3169.6	0.0	0.0	100.28	0.0
MagicTelescope	Neural-CBP	3370.36	1.0	16.0	496.68	1.0
MagicTelescope	IneurAL (official)	7343.04	0.0	0.0	6452.8	0.0
MagicTelescope	IneurAL (less exploration)	4473.2	0.0	0.0	3138.28	0.0
MagicTelescope	Neuronal (official)	4226.96	0.002	0.0	2555.96	0.0
MagicTelescope	Neuronal (less exploration)	3372.2	0.994	4.0	556.52	0.631
MagicTelescope	Cesa	3245.64	0.623	3.0	328.76	0.033
MagicTelescope	Margin	3574.12	0.483	2.0	58.04	0.0
adult	Neural-CBP	2968.88	1.0	10.0	127.64	1.0
adult	IneurAL (official)	8243.12	0.0	0.0	7610.2	0.0
adult	IneurAL (less exploration)	3909.48	0.027	2.0	1136.24	0.0
adult	Neuronal (official)	4819.44	0.001	1.0	3395.52	0.0
adult	Neuronal (less exploration)	2523.64	0.155	3.0	305.96	0.032
adult	Cesa	3180.0	0.643	3.0	320.12	0.001
adult	Margin	3166.56	0.682	6.0	19.92	0.0

Table 3: Supplement for Figure 5. Neuronal with $\mu_1 = \mu_2 = 0.0001$. Mean regret: average regret at the last step ($T = 10k$). P-value: Welch’s t-test on the distribution of regrets at the last step, with NeuralCBP as reference (p-value > 0.05 means no statistical difference). Win count: number of times a given strategy achieved the lowest final regret (ties included). Mean exploration: average number of expert-verified observations. P-value (exploration): Welch’s t-test on the distribution of number of expert queries.

Dataset	Approach	Mean regret	p-value	win count	Mean Exploration	p-value (exploration)
MNIST	Neural-CBP	1811.96	1.0	25.0	1305.24	1.0
MNIST	IneurAL (official)	4016.84	0.0	0.0	3870.12	0.0
MNIST	IneurAL (less exploration)	2371.36	0.0	0.0	1818.56	0.0
MNIST	Neuronal (official)	3275.0	0.0	0.0	3224.84	0.0
MNIST	Neuronal (less exploration)	2213.16	0.0	0.0	2030.44	0.0
Fashion	Neural-CBP	2898.24	1.0	25.0	1523.92	1.0
Fashion	IneurAL (official)	4882.48	0.0	0.0	4382.88	0.0
Fashion	IneurAL (less exploration)	3437.76	0.0	0.0	2210.2	0.0
Fashion	Neuronal (official)	4466.76	0.0	0.0	4193.28	0.0
Fashion	Neuronal (less exploration)	3417.44	0.0	0.0	2777.44	0.0
covertypes	Neural-CBP	5060.24	1.0	12.0	446.96	1.0
covertypes	IneurAL (official)	9129.68	0.0	0.0	8235.72	0.0
covertypes	IneurAL (less exploration)	7707.72	0.0	0.0	4862.12	0.0
covertypes	Neuronal (official)	5970.96	0.0	0.0	4802.48	0.0
covertypes	Neuronal (less exploration)	5060.92	0.997	13.0	1330.4	0.001
shuttle	Neural-CBP	907.56	1.0	14.0	190.08	1.0
shuttle	IneurAL (official)	7989.88	0.0	0.0	7901.0	0.0
shuttle	IneurAL (less exploration)	2810.08	0.0	1.0	2292.48	0.0
shuttle	Neuronal (official)	1547.08	0.004	7.0	183.48	0.902
shuttle	Neuronal (less exploration)	1524.0	0.003	4.0	157.16	0.437

Table 4: Numeric values in support of Section 5.2 presented in the main paper (see Figure 2). `Neuronal` with $\mu_1 = \mu_2 = 0.001$. Mean regret: average regret at the last step ($T = 10k$). P-value: Welch’s t-test on the distribution of regrets at the last step, with `NeuralCBP` as reference (p-value > 0.05 means no statistical difference). Win count: number of times a given strategy achieved the lowest final regret (ties included). Mean exploration: average number of expert-verified observations. P-value (exploration): Welch’s t-test on the distribution of number of expert queries.

Dataset	Approach	Mean regret	p-value	win count	Mean Exploration	p-value (exploration)
MNIST	Neural-CBP	1811.96	1.0	25.0	1305.24	1.0
MNIST	IneurAL (official)	4016.84	0.0	0.0	3870.12	0.0
MNIST	IneurAL (less exploration)	2371.36	0.0	0.0	1818.56	0.0
MNIST	Neuronal (official)	4123.8	0.0	0.0	4093.68	0.0
MNIST	Neuronal (less exploration)	2722.72	0.0	0.0	2605.16	0.0
Fashion	Neural-CBP	2898.24	1.0	25.0	1523.92	1.0
Fashion	IneurAL (official)	4882.48	0.0	0.0	4382.88	0.0
Fashion	IneurAL (less exploration)	3437.76	0.0	0.0	2210.2	0.0
Fashion	Neuronal (official)	4881.16	0.0	0.0	4709.56	0.0
Fashion	Neuronal (less exploration)	3584.28	0.0	0.0	3089.64	0.0
covertypes	Neural-CBP	5060.24	1.0	20.0	446.96	1.0
covertypes	IneurAL (official)	9129.68	0.0	1.0	8235.72	0.0
covertypes	IneurAL (less exploration)	7707.72	0.0	0.0	4862.12	0.0
covertypes	Neuronal (official)	7831.48	0.0	0.0	7287.32	0.0
covertypes	Neuronal (less exploration)	5659.96	0.0	4.0	3431.8	0.0
shuttle	Neural-CBP	907.56	1.0	20.0	190.08	1.0
shuttle	IneurAL (official)	7989.88	0.0	0.0	7901.0	0.0
shuttle	IneurAL (less exploration)	2810.08	0.0	0.0	2292.48	0.0
shuttle	Neuronal (official)	1661.08	0.0	1.0	1277.04	0.0
shuttle	Neuronal (less exploration)	1666.0	0.0	4.0	404.56	0.011

Table 5: Numeric values in support of Figure 6. `Neuronal` with $\mu_1 = \mu_2 = 0.0001$. Mean regret: average regret at the last step ($T = 10k$). P-value: Welch’s t-test on the distribution of regrets at the last step, with `NeuralCBP` as reference (p-value > 0.05 means no statistical difference). Win count: number of times a given strategy achieved the lowest final regret (ties included). Mean exploration: average number of expert-verified observations. P-value (exploration): Welch’s t-test on the distribution of number of expert queries.

Dataset	Approach	Mean regret	p-value	win count	Mean Exploration	p-value (exploration)
MNIST	Neural-CBP	954.458	1.0	17.0	439.75	1.0
MNIST	Neuronal (official)	1342.24	0.0	0.0	1284.16	0.0
MNIST	Neuronal (less exploration)	992.6	0.015	7.0	817.92	0.0
Fashion	Neural-CBP	2749.72	1.0	20.0	606.52	1.0
Fashion	Neuronal (official)	3576.76	0.0	0.0	3027.96	0.0
Fashion	Neuronal (less exploration)	2818.8	0.072	6.0	1698.16	0.0
CIFAR10	Neural-CBP	6865.92	1.0	25.0	2515.04	1.0
CIFAR10	Neuronal (official)	8535.76	0.0	0.0	7519.36	0.0
CIFAR10	Neuronal (less exploration)	7478.12	0.0	0.0	5114.48	0.0

Table 6: Numeric values in support of Section 5.2 presented in the main paper (see Figure 3). *Neuronal* with $\mu_1 = \mu_2 = 0.001$. Mean regret: average regret at the last step ($T = 10k$). P-value: Welch’s t-test on the distribution of regrets at the last step, with *NeuralCBP* as reference (p-value > 0.05 means no statistical difference). Win count: number of times a given strategy achieved the lowest final regret (ties included). Mean exploration: average number of expert-verified observations. P-value (exploration): Welch’s t-test on the distribution of number of expert queries.

Dataset	Approach	Mean regret	p-value	win count	Mean Exploration	p-value (exploration)
MNIST	Neural-CBP	954.458	1.0	24.0	439.75	1.0
MNIST	Neuronal (official)	2009.04	0.0	0.0	1975.8	0.0
MNIST	Neuronal (less exploration)	1274.24	0.0	0.0	1154.96	0.0
Fashion	Neural-CBP	2749.72	1.0	24.0	606.52	1.0
Fashion	Neuronal (official)	4182.96	0.0	0.0	3919.52	0.0
Fashion	Neuronal (less exploration)	3095.28	0.0	1.0	2352.64	0.0
CIFAR10	Neural-CBP	6865.92	1.0	25.0	2515.04	1.0
CIFAR10	Neuronal (official)	9410.12	0.0	0.0	9130.44	0.0
CIFAR10	Neuronal (less exploration)	8483.68	0.0	0.0	6674.24	0.0

Table 7: Numeric values in support of Figure 7. *Neuronal* with $\mu_1 = \mu_2 = 0.0001$. Mean regret: average regret at the last step ($T = 10k$). P-value: Welch’s t-test on the distribution of regrets at the last step, with *NeuralCBP* as reference (p-value > 0.05 means no statistical difference). Win count: number of times a given strategy achieved the lowest final regret (ties included). Mean exploration: average number of expert-verified observations. P-value (exploration): Welch’s t-test on the distribution of number of expert queries.